Genetic and Cellular Architecture of Breast Cancer Risk in Multi-Ancestry Studies of 159,297 Cases and 212,102 Controls

James L. Li[1,*], Maria Zanti[2,*], Jacob Williams[3,*], Om Jahagirdar[3], Guochong Jia[4], Alistair Turcan[5], Qiang Hu[6], Jean-Tristan Brandenburg[7,8], Li Yan[6], Weang-Kee Ho[9,10], Jingmei Li[11], José Patricio Miranda[12,13,14], Devika Godbole[3], Julie-Alexia Dias[15], Xiaomeng Zhang[16], Leila Dorling[16], Wenlong Carl Chen[7,8,40], Nicholas Boddicker[17], Ying Wang[18], Alicia Martin[18,19,20], Yan Dora Zhang[21], Joe Dennis[16], Esther M. John[22,23], Gabriela Torres-Mejia[24], Larry Kushi[25,26], Jeffrey Weitzel[27], Susan L. Neuhausen[28], Luis Carvajal-Carmona[29,30], Christopher Haiman[31], Elad Ziv[32], Laura Fejerman[33,34,35], Wei Zheng[4], Dezheng Huo[1], Douglas Easton[16,36], Stephen J. Chanock[3], Nilanjan Chatterjee[37,38], Peter Kraft[3], Montserrat Garcia-Closas[39], Wendy S.W. Wong[3], Kyriaki Michailidou[2], Qianqian Zhu[6], Martin Jinye Zhang[5], Diptavo Dutta[3], Thomas U. Ahearn[3,†], Haoyu Zhang[3,†]

[1] Department of Public Health Sciences, University of Chicago, Chicago, IL, USA

[2] Biostatistics Unit, The Cyprus Institute of Neurology and Genetics, Nicosia, Cyprus

[3] Division of Cancer Epidemiology and Genetics, National Cancer Institute, National Institutes of Health, Bethesda, MD, USA

[4] Division of Epidemiology, Department of Medicine, Vanderbilt Epidemiology Center, Vanderbilt-Ingram Cancer Center, Vanderbilt University Medical Center, Nashville, TN, USA

[5] Ray and Stephanie Lane Computational Biology Department, School of Computer Science, Carnegie Mellon University, Pittsburgh, PA, USA

[6] Department of Biostatistics and Bioinformatics, Roswell Park Comprehensive Cancer Center, Buffalo, NY, USA

[7] Sydney Brenner Institute for Molecular Bioscience, Faculty of Health Sciences, University of the Witwatersrand, Johannesburg, South Africa

[8] Strengthening Oncology Services Research Unit, Faculty of Health Sciences, University of the Witwatersrand, Johannesburg, South Africa

[9] School of Mathematical Sciences, Faculty of Science and Engineering, University of Nottingham Malaysia, Semenyih, Selangor, Malaysia

[10] Cancer Research Malaysia, Subang Jaya, Selangor, Malaysia

[11] Genome Institute of Singapore, Agency for Science, Technology and Research (A*STAR), Singapore

[12] Department of Nutrition, Diabetes and Metabolism, School of Medicine, Pontificia Universidad Católica de Chile, Santiago, Chile

[13] PhD Program in Epidemiology, Pontificia Universidad Católica de Chile, Santiago, Chile

[14] Advanced Center for Chronic Diseases, Pontificia Universidad Católica de Chile & Universidad de Chile, Santiago, Chile

[15] Department of Biostatistics, Harvard T.H. Chan School of Public Health, Boston, MA, USA

[16] Centre for Cancer Genetic Epidemiology, Department of Public Health and Primary Care, University of Cambridge, Cambridge, UK

[17] Department of Quantitative Health Sciences, Mayo Clinic, Rochester, MN, USA

[18] Analytic and Translational Genetics Unit, Massachusetts General Hospital, Boston, MA, USA

[19] Department of Medicine, Harvard Medical School, Boston, MA, USA

[20] Stanley Center for Psychiatric Research, Broad Institute of MIT and Harvard, Cambridge, MA, USA

[21] Department of Statistics & Actuarial Science, School of Computing and Data Science, The University of Hong Kong, Hong Kong SAR, China

[22] Departments of Epidemiology & Population Health and of Medicine (Oncology), Stanford University School of Medicine, Stanford, CA, USA

56 [23] Stanford Cancer Institute, Stanford University School of Medicine, Stanford, CA, USA

57 [24] Instituto Nacional de Salud Pública, Cuernavaca, Mexico

58 [25] UC Davis Genome Center, University of California, Davis, Davis, CA, USA

59 [26] Division of Research, Kaiser Permanente Northern California, Oakland, CA, USA

60 [27] Division of Precision Prevention, University of Kansas Comprehensive Cancer
61 Center, Kansas City, KS, USA

62 [28] Department of Population Sciences, Beckman Research Institute of City of Hope,
63 Duarte, CA, USA

64 [29] Department of Biochemistry and Molecular Medicine, School of Medicine, University
65 of California at Davis, Davis, CA, USA

66 [30] The Health Equity, Leadership, Science and Community Laboratory, Genome Center,
67 University of California at Davis, Davis, CA, USA

68 [31] Department of Preventive Medicine, Norris Comprehensive Cancer Center, Keck
69 School of Medicine, University of Southern California, Los Angeles, CA, USA

70 [32] Division of General Internal Medicine, Department of Medicine, University of
71 California, San Francisco, San Francisco, CA, USA

72 [33] Department of Public Health Sciences, University of California Davis, Davis, CA, USA

73 [34] Genome Center, University of California Davis, Davis, CA, USA

74 [35] UC Davis Comprehensive Cancer Center, University of California Davis, Davis, CA,
75 USA

76 [36] Centre for Cancer Genetic Epidemiology, Department of Oncology, University of
77 Cambridge, Cambridge, UK

78 [37] Department of Biostatistics, Johns Hopkins University, Baltimore, MD, USA

79 [38] Department of Oncology, Johns Hopkins School of Medicine, Baltimore, MD, USA

80 [39] Cancer Epidemiology and Prevention Research Unit, The Institute of Cancer
81 Research and Imperial College London, London, UK

82 [40] National Cancer Registry, a Division of the National Institute for Communicable
83 Diseases, National Health Laboratory Service, Johannesburg, South Africa

84

85 [*]These authors equally contributed to the manuscript

86 [†]Correspondence to: Thomas U. Ahearn (thomas.ahearn@nih.gov), and Haoyu Zhang
87 (haoyu.zhang2@nih.gov).

88

SUMMARY

Breast cancer genome-wide association studies (GWAS) have identified over 200 independent genome-wide significant susceptibility markers. However, most studies have focused on one or two ancestral groups. We examined breast cancer genetic architecture using GWAS summary statistics from African (AFR), East Asian (EAS), European (EUR) and Hispanic/Latina (H/L) samples, totaling 159,297 cases and 212,102 controls, comprising the largest multi-ancestry study of breast cancer to date. The logit-scale heritability of breast cancer ranged from h^2=0.47 (SE = 0.07) in EAS to AFR h^2=0.61 (SE = 0.10), with no significant differences across ancestries (p=0.63). The estimated number of susceptibility markers in a sparse normal-mixture effects model also varied from 4,446 (SE = 3,100) in EAS to 8,308 (SE = 2,751) in AFR, but differences were not significant across ancestries (p=0.55). Cross-sample genetic correlations varied, with the strongest correlation between EUR and EAS ($\rho = 0.79$, SE = 0.08) and weakest between AFR and H/L ($\rho = 0.26$, SE = 0.24). Common variants in regulatory elements were enriched for genetic association across samples. By integrating the GWAS summary statistics with the Tabula Sapiens scRNA-seq atlas, we identified ancestry-shared associations between breast cancer and specific cell types, including innate immune cells, secretory epithelial cells and stromal cells. Collectively, these results support a largely shared polygenic architecture of breast cancer across ancestries, with consistent enrichment of common regulatory variants and convergent cellular signatures identified through single-cell analyses.

INTRODUCTION

Breast cancer is the most common cancer among women worldwide, affecting over two million individuals annually[1]. Genome-wide association studies (GWAS) have identified more than 200 genome-wide significant susceptibility markers associated with breast cancer risk[2–7]. However, most GWAS have focused on populations of European (EUR) and East Asian (EAS) ancestry samples[2,4–9], while studies in African (AFR) [3,10–13] and Hispanic/Latina (H/L)[14,15] samples are limited, and often with smaller sample sizes. Existing studies have both replicated risk markers identified across ancestry populations, as well as identified population-specific risk markers. Furthermore, polygenic risk score (PRS) models trained in European samples often exhibit lower predictive performance in other genetic ancestry samples[16], emphasizing the need for a broader understanding of breast cancer genetics across different ancestries.

We examined the genetic architecture of breast cancer using GWAS summary statistics from a total of 159,297 cases and 212,102 controls from AFR, EAS, EUR and H/L samples (**Supplementary Figure 1, Supplementary Table 1**). We estimated genome-wide single-nucleotide polymorphism (SNP)-based heritability, the number of susceptibility genetic markers, and assessed genetic correlations across samples. We further investigated enrichment of regulatory elements associated with breast cancer risk, and applied the single-cell disease-relevance score (scDRS+) method to identify cell types implicated in breast cancer across ancestry samples. These findings further refine our understanding of breast cancer genetics and highlight the influence of common variants and regulatory elements across ancestries.

RESULTS

Logit-scale SNP-based heritability

We used linkage-disequilibrium (LD) score regression[17] to estimate the logit-scale SNP-based heritability (h^2), which quantifies the proportion of variance in the log-odds of disease explained by common genetic variants under a logistic regression model (**Methods**). To obtain a robust estimate of the heritability, we conducted sensitivity

analyses by applying various SNP inclusion criteria, including different minor allele frequency thresholds (MAF > 0.01 or MAF > 0.05), and SNP arrays (HapMap3[18] or HapMap3 + Multi-Ethnic Genotyping Array (MEGA)[19]). LD scores were computed using 1000 Genomes Project (1000G)[20] Phase 3 for AFR, EAS and EUR samples, and Admixed American (AMR) as reference for H/L samples. For AFR, we additionally generated estimates using a subset of 2,731 controls from the African Ancestry Breast Cancer Genetics (AABCG) Consortium.

Heritability estimates for EUR and EAS samples remained consistent across different SNP inclusion criteria hat varied by minor allele frequency thresholds (MAF > 0.01 vs. MAF > 0.05) and SNP sets (HapMap3 vs. HapMap3 + MEGA) (**Supplementary Table 2**). Thus, we adopted the most comprehensive SNP set (MAF > 0.01 and HapMap3 plus MEGA SNPs) for our final analyses. In contrast, heritability estimates for AFR varied significantly depending on the LD reference panel (h^2 =0.27, SE=0.11 to h^2 =0.61, SE=0.10; **Supplementary Table 2)**. Given that the GWAS summary statistics for AFR were primarily from U.S. samples (85.3%)[12], while AFR in 1000G are mostly from African continental samples, AABCG likely provides more appropriate reference for LD estimation in this context. For H/L, heritability estimates were less stable due to the smaller GWAS sample size, leading to larger standard errors. To enhance robustness, we applied the more conservative MAF > 0.05 threshold.

Across ancestry samples, SNP-based heritability estimates ranged from EAS h^2=0.466 (SE=0.066) to AFR h^2=0.614 (SE=0.095), with EUR h^2=0.501 (SE=0.050) and H/L h^2=0.588 (SE=0.360) showing intermediate values (**Table 1**). While point estimates varied modestly, we found no statistically significant evidence of heterogeneity in SNP-based heritability across ancestry samples (Cochran's Q = 1.72, p = 0.63, **Supplementary Figure 2**). Overall, these findings suggest common susceptibility variants moderately contribute to breast cancer risk across samples. The slightly higher point estimate in AFR could reflect the broader range of genetic variation captured by a larger set of well-imputed SNPs (n=1,628,778) (**Table 1**).

The polygenicity of breast cancer

Breast cancer exhibits a high degree of polygenicity across populations. Using the GENESIS package[21,22], we modeled the distribution of marker effect sizes for AFR, EAS and EUR samples as a sparse mixture of normal. Due to a limited sample size, the model for H/L did not converge, precluding a reliable estimate. Across the three analyzed samples, marker effect sizes showed no evidence of inflation (**Supplementary Figure 3**). The estimated polygenicity (number of markers with non-zero effects) was highest in AFR (8,308, SE=2,751), followed by EUR (5,235, SE=1,191) and EAS (4,446, SE=3,100, **Supplementary Table 3**). We found no statistically significant heterogeneity in polygenicity across samples (Cochran's Q = 1.20, p = 0.55), that observed differences are consistent with sampling variation. These findings support a broadly shared polygenic basis of breast cancer across ancestries, with modest differences that may reflect sample-specific power or LD structure.

We used GENESIS to project the proportion of heritability explained and the accuracy of polygenic risk scores (PRS) at increasing GWAS sample sizes (**Figure 1A, Supplementary Table 4**). Polygenic risk scores evaluated in GENESIS were based on the clumping and thresholding (CT-PRS) approach[23,24], applied independently to each sample using ancestry-specific GWAS summary statistics and corresponding LD reference panels. The proportion of genetic variance explained was defined as the variance captured by the CT-PRS divided by the logit-scale heritability of common variants. At a GWAS sample size of 100,000 cases and 100,000 controls, the proportion of genetic variance explained was 26.2% in AFR, 39.4% in EAS, and 38.6% in EUR (**Supplementary Table 4**). Projected area under the curve (AUC) values for CT-PRS followed a similar trend. At a sample size of 100,000 cases and 100,000 controls, the expected AUC was 61.1% for AFR, 63.4% for EAS and 62.1% for EUR (**Figure 1B, Supplementary Table 4**). Asymptotically (i.e., at infinite sample size), the estimated maximum AUCs for CT-PRS were 71% for AFR, and 71% for EAS, and 69% for EUR (**Supplementary Table 3**).

Cross-sample genetic correlations of breast cancer

We next assessed cross-sample genetic correlations of breast cancer using *Popcorn*[25], which estimates genetic effect correlations accounting for LD differences across ancestries. Using variants from the HapMap3 panel, we identified the strongest genetic correlations between EUR and EAS (ρ: 0.79, SE: 0.08) and EUR and H/L (ρ: 0.68, SE: 0.21), indicating substantial shared genetic architecture between these samples (**Figure 2A, Supplementary Table 5**). In contrast, genetic correlations involving AFR were consistently lower, with estimates ranging from AFR and H/L (ρ = 0.26, SE = 0.24) to AFR and EUR (ρ = 0.42, SE = 0.14), suggesting greater divergence in effect sizes of variants tagging in AFR. We further evaluated whether expanding the variant set to include both HapMap3 and MEGA array variants altered correlation patterns and the estimates remained broadly consistent (**Figure 2B, Supplementary Table 5**).

Genomic enrichment of breast cancer heritability

To investigate the regulatory landscape underlying breast cancer heritability, we estimated the proportion of SNP-based heritability attributable to 73 functional genomic annotations using stratified LD-score regression[26,27] (**Methods**, **Supplementary Table 6**). These annotations, based on the baseline-LD v2.2 model, include a curated set of coding, regulatory, and evolutionary genomic features previously shown to capture trait heritability[26–28]. Annotations definitions and data sources are described in the **Methods**. In the EUR sample, several annotations showed strong, statistically significant enrichment. The highest enrichment was found in ancient promoter regions (32.42-fold, $p = 1.98 \times 10^{-4}$), followed by transcription factor binding sites (TFBS) (5.79-fold, $p = 9.16 \times 10^{-5}$), and the promoter-associated histone mark H3K4me3 (4.9-fold, $p = 8.56 \times 10^{-5}$). We also observed significant enrichment in super-enhancers (3.01-fold, $p = 3.73 \times 10^{-11}$), and enhancer-associated marks H3K4me1 (2.52-fold, $p = 1.28 \times 10^{-7}$) and H3K27ac (2.16-fold, $p = 2.25 \times 10^{-10}$), highlighting the contribution of regulatory elements to genetic risk. In the EAS sample, the only annotation reaching statistical significance after Bonferroni correction ($p < 6.84 \times 10^{-4}$) was super-enhancers (2.73-fold, $p = 2.6 \times 10^{-7}$). In the AFR sample, significant enrichment was found for H3K27ac (2.15-fold, $p = 2.59 \times 10^{-4}$). No statistically significant enrichment was observed in the H/L sample. Patterns of

225 enrichment for annotations that were significantly enriched in at least one ancestry
226 sample were generally consistent across ancestries (**Supplementary Figure 4**). A
227 heterogeneity test across samples for these five annotations revealed no statistically
228 significant differences after Bonferroni correction.

229 **Cell-type specific associations with breast cancer risk**

230 To identify cell types associated with breast cancer risk across ancestries, we applied
231 scDRS+[29,30], to GWAS summary statistics from each ancestry and the Tabula Sapiens
232 scRNA-seq atlas[31] (133 cell types across 24 tissues). scDRS+ computes disease
233 relevance score for individual cells based on expression of GWAS-prioritized genes,
234 then aggregates these scores to test cell-type enrichments. For robustness, we
235 prioritized cell types showing associations in more than three ancestry samples for
236 robustness, reporting both fine-mapped (**Figure 3A, Supplementary Table 7**) and
237 marginal results (**Figure 3B; Supplementary Table 8**).

238 First, we observed associations in several innate immune cell types, including classical
239 monocytes (false discovery rate (FDR) <0.05 in EAS and EUR; FDR<0.1 in H/L and
240 AFR, **Figure 3A**) and neutrophils (FDR<0.05 in EAS; FDR<0.1 in H/L and EUR, **Figure**
241 **3A**), consistent with the established role of myeloid cells in breast cancer biology and
242 the tumor microenvironment[32–37]. Second, we detected associations for lacrimal gland
243 functional unit cells (FDR<0.05 in EAS and EUR; FDR<0.1 in H/L and AFR, **Figure 3A**)
244 and skeletal muscle satellite stem cells (FDR<0.05 in EAS and EUR; FDR<0.1 in H/L,
245 **Figure 3A**). These associations are unlikely to reflect direct etiological cell types for
246 breast cancer but may instead arise from shared epithelial or stromal regulatory
247 programs in mammary tissue. For example, luminal epithelial cells of mammary gland
248 were non-significant in fine-mapping but showed marginal association (FDR<0.05 in
249 AFR; FDR≈0.07-0.10 for EAS, EUR, and H/L, **Supplementary Table 8**), while
250 fibroblasts of breast were likewise non-significant in fine-mapping but displayed
251 marginal associations in EAS (FDR=0.049), H/L (FDR=0.02), and AFR (FDR=0.008),
252 with a weaker signal in EUR (FDR=0.11). Third, these findings are supported by
253 consistent marginal association signals across all samples (**Figure 3B**), which we

included to mitigate the interpretative challenges inherent in fine-mapping correlated cell populations.

To assess shared cellular signatures across ancestry samples, we examined the correlation of marginal scDRS+ association scores for the key cell types, neutrophils, classical monocytes, and skeletal muscle satellite stem cells. The association scores for these cell types were highly correlated between ancestry pairs (**Supplementary Figure 5**), suggesting conserved cellular mechanisms underlying genetic susceptibility. UMAP visualizations further demonstrated overlapping disease-relevant cell clusters across samples (**Figure 3C, D**).

DISCUSSION

We present a compressive cross-ancestry evaluation of the genetic architecture of breast cancer using large-scale GWAS summary statistics from AFR, EAS, EUR and H/L samples. With 220,498 cases and 200,182 controls, this is the largest such evaluation to date. Our results support a largely shared polygenic architecture of breast cancer across ancestries, with consistent enrichment of common regulatory variants and convergent cellular signatures identified through single-cell analyses. While point estimates of heritability and polygenicity varied across samples, we did not detect statistically significant heterogeneity, suggesting that observed differences likely reflect sampling variation, LD structure, or reference panel choice rather than fundamental biological divergence.

Breast cancer exhibited moderate logit-scale SNP-based heritability across all groups, with the highest point estimate observed in AFR. These estimates were robust in EUR and EAS, but more sensitive to LD reference panel choice in AFR, where using sample-matched LD from AABCG controls significantly increased heritability compared to using AFR from 1000G (**Supplementary Table 2**). This highlights the importance of appropriate ancestry-specific LD modeling in admixed populations[38–40]. While the point estimates varied, our formal test of heterogeneity found no statistically significant differences in heritability across samples (p=0.64). These results are broadly consistent with prior reports based on subsets of our underlying data. For example, Michailidou et al. (2017)[7], using primarily OncoArray data (a large component of our EUR sample),

285 estimated that common variants explained ~41% of the familial relative risk,
286 corresponding to a logit-scale heritability of approximately 0.568, closely matching our
287 EUR estimate of 0.501. Likewise, our AFR estimate of 0.614 is comparable to the logit-
288 scale heritability (referred to as frailty-scale) of 0.667 reported in the recent African
289 ancestry sample breast cancer GWAS[12], which used the same summary statistics but a
290 different LD reference panel. While heritability has been estimated in prior studies,
291 these have largely focused on individual ancestry groups and used varying
292 methodologies; to our knowledge, our study provides the first systematic, cross-
293 ancestry comparison of logit-scale SNP-based heritability using harmonized models.
294 We focused on the logit scale, as it provides an interpretable and robust estimate of
295 genetic variance explained by GWAS variants and connects directly to familial risk[41],
296 without requiring assumptions about disease prevalence.
297

298 We also observed a high degree of polygenicity across ancestry samples. The
299 estimated number of susceptibility markers with non-zero effects in a sparse mixture
300 model ranged from 4,446 in EAS to 8,308 in AFR. While these differences may reflect
301 true biological variation, such as lower LD in African genomes allowing more markers to
302 be distinguished statistically, our heterogeneity test found no significant differences in
303 polygenicity across samples (p=0.55). Interestingly, the AFR sample also had the
304 highest SNP-based heritability estimate, suggesting a potentially larger contribution of
305 common variants to risk. However, PRS performance in AFR remained lower compared
306 to EUR and EAS at comparable sample sizes[42]. This finding is consistent with our
307 projections (**Figure 1B**), which demonstrate that PRS accuracy is not only a function of
308 total heritability, but also of the effect-size distribution, i.e., the degree of polygenicity,
309 and the LD structure of the population. Thus, the higher heritability in AFR may be offset
310 by greater polygenicity and LD complexity, both of which reduce the efficiency of risk
311 prediction models based on common variants.

312 Genetic correlations were strongest between EUR and EAS ($\rho = 0.79$), and weakest for
313 comparison involving AFR, reflecting ancestral differences in LD structure and variant
314 tagging. These findings may reflect known patterns of human migration and population
315 divergence indicated from populations genetics, including an initial divergence in line

316 with the “Out-of-Africa” migration model, with subsequent and more recent separation
317 between European, East Asian, and American populations[43]. The moderately strong
318 correlation between EUR and H/L ($\rho = 0.68$) likely reflects the substantial European
319 ancestry present in many H/L individuals. However, it is important to note that this
320 average may obscure heterogeneity within H/L populations: individuals with higher
321 proportions of Indigenous American ancestry would be expected to show lower genetic
322 correlation with EUR populations. The H/L summary statistics analyzed here were
323 derived from both U.S.-based cohorts (e.g., NC-BCFR/SFBCS, RPGEH, MEC) and
324 Latin American studies (COLUMBUS and CAMA), encompassing a mix of Mexican,
325 Central American, and South American individuals with variable proportions of
326 European, Indigenous American, and African ancestry. Similarly, the AFR GWAS data
327 primarily reflect African-American individuals with admixed West African and European
328 ancestry. As such, the estimated genetic correlations represent average effect-size
329 sharing across ancestrally diverse groups and may mask finer-scale heterogeneity.
330 Future analyses incorporating local ancestry or ancestry-stratified GWAS may help to
331 disentangle these layered genetic relationships more precisely.

332 Stratified heritability enrichment revealed consistent contributions from regulatory
333 elements, including promoters, enhancers, and histone marks (e.g., H3K27ac,
334 H3K4me1), across ancestry samples. While some differences in the strength of
335 enrichment were observed, heterogeneity tests did not identify statistically significant
336 variation in enrichment patterns across samples. In the H/L sample, no annotations
337 reached statistical significance, likely due to limited GWAS sample size and reduced
338 power to detect enrichment.

339 Integrating GWAS with single-cell transcriptomic data via scDRS+[29], we identified
340 consistent enrichments in classical monocytes, neutrophils, lacrimal gland functional
341 unit cell, and skeletal muscle satellite stem cells for breast cancer-associated gene
342 expression across ancestries. These findings suggest that genetic risk variants may
343 exert their effects through immune, epithelial, and stromal cells, such as inflammation,
344 innate immune responses, or tissue repair, rather than solely within breast epithelial
345 cells. Monocyte and neutrophil associations align with prior evidence of myeloid roles in
346 tumor inflammation and progression [32–37]. The lacrimal gland functional unit cells and

347 skeletal muscle satellite stem cell associations are unlikely to reflect direct etiological
348 cell types for breast cancer but may instead arise from shared epithelial or stromal
349 regulatory programs in mammary tissue , such as those observed for luminal epithelial
350 cells of mammary gland (FDR<0.05 in EAS; FDR<0.2 in EUR and AFR) and fibroblasts
351 of breast (non-significant in fine-mapping but showing marginal association at
352 FDR<0.05 in EAS,H/L and AFR). Alternatively, they could support emerging roles for
353 muscle or stromal niches in metastatic reactivation [44]. While scDRS+ does not directly
354 identify the tissue of origin, it provides a hypothesis-generating framework that links
355 genetic risk to specific cellular contexts based on expression profiles. The cross-
356 ancestry consistency reinforces shared biological pathways underlying breast cancer
357 risk in diverse populations.

358 This is the largest cross-ancestry investigation of breast cancer architecture; however,
359 our study was limited by relatively small sample sizes particularly in non-European
360 samples. Our findings highlight the value of large samples from diverse populations in
361 breast cancer GWAS, which enables more powerful modeling of the underlying
362 polygenic risk by leveraging similar and distinct linkage disequilibrium patterns across
363 populations. Notably, important efforts are being made to increase samples size of
364 breast cancer GWAS among women of Hispanic/Latina descent by the Latin American
365 Genomics of Breast Cancer Consortium (LAGENO-BC) and among women of African
366 descent by AABCG[12]. Moreover, the Confluence Project is building a large, diverse
367 research resource of approximately 300,000 breast cancer cases and 300,000 controls
368 by coordinating collaborations between LAGENO-BC, AABCG[12], BCAC, the
369 Consortium of Investigators of Modifiers of BRCA1/2 (CIMBA), the Male Breast Cancer
370 Genetics Consortium (MERGE), and other breast cancer studies and clinical trials, that
371 will help support and lead to an improved understanding of breast cancer etiology, and
372 improvements in risk stratification and prevention across diverse populations. In
373 summary, our study refines the understanding of breast cancer genetics across
374 populations and highlights the value of multi-ancestry studies of breast cancer for
375 gaining better insights in breast cancer etiology and polygenic risk prediction and
376 stratification.

377

378 **Table 1. Sample-specific estimates of the logit-scale SNP-based heritability**

Sample	Cases	Controls	MAF cutoff	LD Score	No. of SNPs	Heritability[e]
AFR[c]	18,034	22,104	MAF > 0.01	AABCG	1,628,778	0.614 (0.095)
EAS[b]	20,393	86,329	MAF > 0.01	1000G	1,189,628	0.466 (0.066)
EUR[a]	118,474	96,201	MAF > 0.01	1000G	1,415,774	0.501 (0.050)
H/L[d]	2,396	7,468	MAF > 0.05	1000G	1,138,603	0.588 (0.360)

Summary statistics from [a]the Breast Cancer Association Consortium (BCAC) (iCOGs and OncoArray) [b] BCAC (OncoArray) and Biobank Japan [c]Summary statistics from the African Ancestry Breast Cancer Genetic (AABCG) consortium [d] NC-BCFR/SFBCS (Northern California Breast Cancer Family Registry/ San Francisco Bay Area Breast Cancer Study), RPGEH (Research project on genes environment and health), MEC (Multiethnic cohort), COLUMBUS and CAMA (Cancer de mama) studies/consortia. Variants included in the analyses were on HapMap3 + Multi-Ethnic Genotyping Array (MEGA). [e] logit-scale heritability (standard error). The logit-scale heritability (also known as frality-scale heritability) is defined as $\sigma^2_{GWAS} = Var(\sum_{m=1}^{M} \beta_m G_m)$, where G_m is the standardized genotype for the mth SNP, β_m is the true log odds ratio for the mth SNP and M is the total number of causal SNPs among the GWAS variants. AFR, African; H/L, Hispanic and Latina; EAS, East Asian; EUR, European; MAF, minor allele frequency; LD, linkage disequilibrium; SNPs, single nucleotide polymorphisms.

379

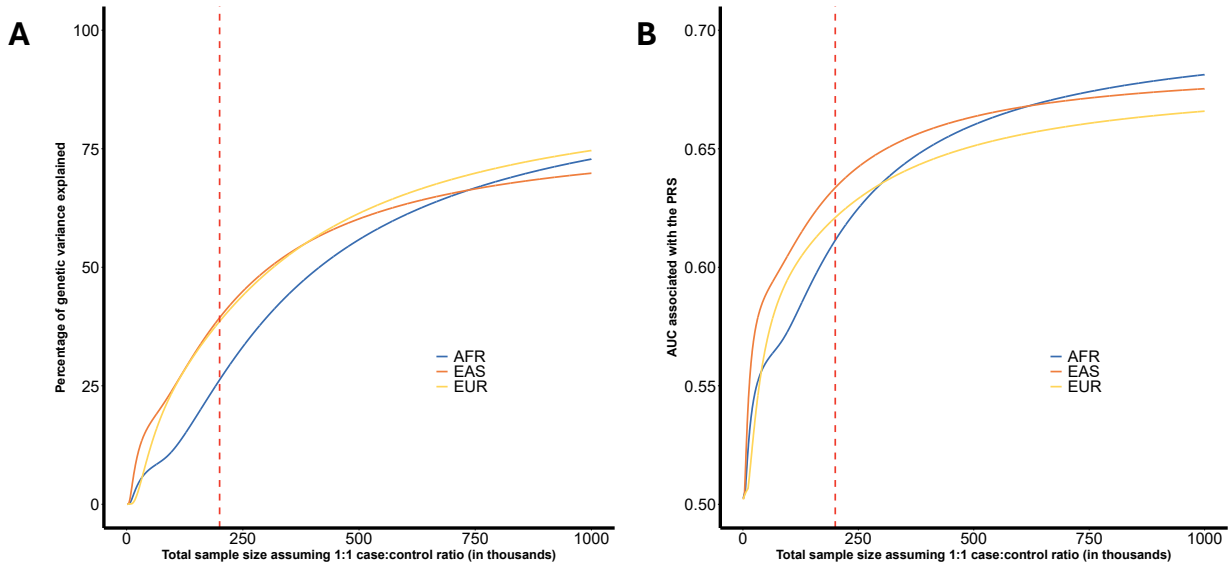

Figure 1. Projected genetic variance explained and predictive performance of clumping and thresholding (CT) polygenic risk scores (PRSs) across samples at varying GWAS sample sizes. A) Estimated proportion of GWAS heritability explained by CT PRS, as a function of total GWAS sample sizes, using the GENESIS framework. The proportion was calculated as the variance explained by the PRS divided by the logit-scale heritability of common variants. B) Projected area under the curve (AUC) for CT PRS models at different sample sizes. Detailed projection of explained genetic variance and AUC at different sample size are provided in **Supplementary Table 4**. The red dashed line indicates a total sample size of 200,000 individuals (100,000 cases and 100,000 controls). Abbreviations: AFR, African; EAS, East Asian; EUR, European.

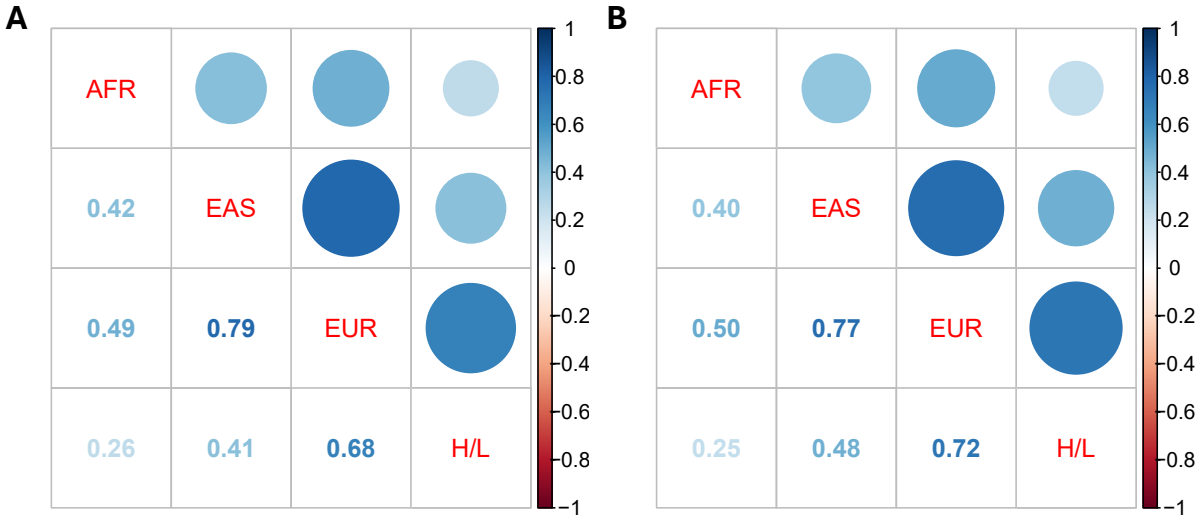

Figure 2. Heatmaps for cross-sample genetic correlations of breast cancer estimated by POPCORN. for A) HapMap3 variants and B) HapMap3 and Multi-Ethnic Genotyping Array variants combined. Note: African, AFR; Hispanic/Latina, H/L; East Asian, EAS; European, EUR.

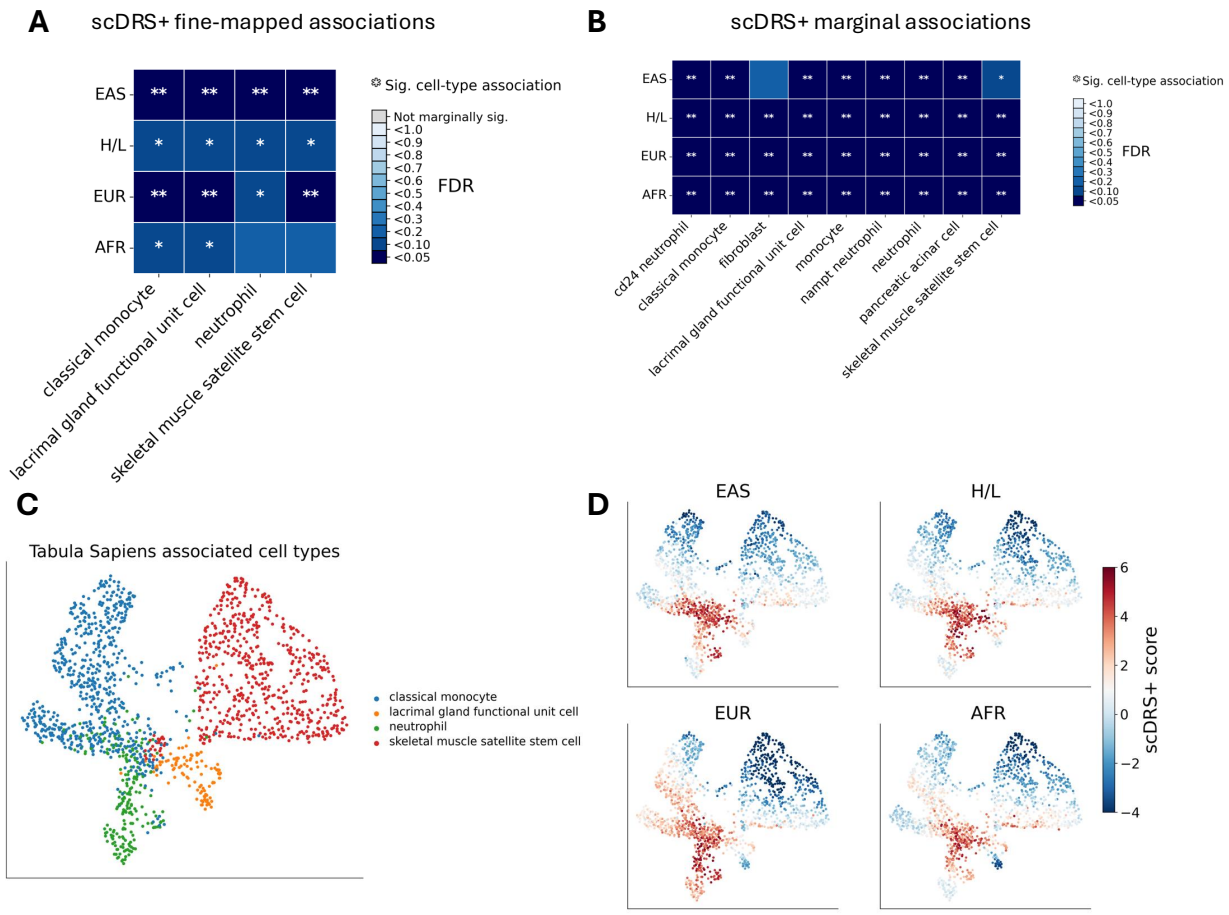

Figure 3: scDRS+ results on Tabula Sapiens. One asterisk indicates FDR<0.1, two asterisks indicates FDR<0.05. A) Fine-mapped associations from scDRS+, showing FDR values for cell types with at least one ancestry having FDR < 0.05; all shown associations are also marginally significant. B) Marginal associations from scDRS+, showing FDR values for cell types with associations across all traits. C) MAP of the cell types shown in panel A. D) UMAPs of scDRS+ scores across ancestries (EAS, EUR, AFR, AMR) for the same cell types as in C. Red indicates higher disease relevance.

412 **METHODS**

413 **Study samples and data collection**

414 We conducted analyses using breast cancer GWAS summary statistics from large
415 genetic consortia focused on AFR, EAS, EUR and H/L samples, with a total of 159,297
416 cases and 212,102 controls across large genetic consortia. Sample labels (AFR, EAS,
417 EUR, H/L) were based on published descriptions of contributing GWAS. For AFR, data
418 were obtained from AABCG, with 18,034 cases and 22,104 controls[12]. For EAS, we
419 conducted a fixed-effect meta-analysis to combine the GWAS summary statistics
420 generated from the BCAC[7] and Biobank Japan[45], comprising a total of 20,393 cases
421 and 86,329 controls. For EUR, we used summary statistics from BCAC (iCOGs and
422 OncoArray) with a combined sample size of 118,474 cases and 96,201 controls[4]. H/L
423 ancestry summary statistics were derived from a meta-analysis of five studies[15]: NC-
424 BCFR/SFBCS (Northern California Breast Cancer Family Registry/ San Francisco Bay
425 Area Breast Cancer Study), RPGEH (Research Program on Genes, Environment and
426 Health), MEC (Multiethnic cohort), COLUMBUS and CAMA (Cancer de mama) including
427 2,396 cases and 7,468 controls. **Supplementary Table 1** summarizes the studies
428 included in the analyses. Processing of meta-analyzed GWAS summary statistics for
429 subsequent analysis is detailed in **Supplementary Figure 1**.

430

431 **Sources of genetic data for LD score construction**

432 We constructed ancestry-specific LD score reference panels using unrelated individuals
433 from Phase 3 of the 1000G[20], excluding first- and second-degree relatives as well as
434 individuals with first-cousin-level relatedness due to inbreeding[46]. For the EUR, EAS,
435 and H/L samples, LD scores were computed using 484 EUR, 480 EAS, and 317 AMR
436 individuals in the 1000G reference panel, respectively. For the AFR sample, we
437 estimated LD scores using a set of 2,730 AFR women controls from the AABCG
438 consortium. As a sensitivity analysis, we also generated LD scores using 575 AFR
439 individuals from 1000G for comparison. The LD scores were conducted using LDSC
440 with a LD window of 1MB using the flag “--l2 --ld-window-kb 1000”.

441 **Estimating ancestry-specific heritability of breast cancer**

442 We estimated the logit-scale sample-specific SNP-based heritability for overall breast
443 cancer risk using LD score regression[17] and using the ancestry-sample-specific GWAS
444 summary statistics. On the logit scale, heritability is defined as: $\sigma^2_{GWAS} =$
445 $Var(\sum_{m=1}^{M} \beta_m G_m)$, where G_m is the standardized genotype for the mth SNP, β_m is the
446 underlying log odds ratio, and M is the total number of causal SNPs among the GWAS
447 variants. This quantity, also referred to as frailty-scale heritability, represents the
448 variance in log-odds of disease explained by common genetic variants. To estimate the
449 logit-scale heritability using LD-score regression, we computed the effective sample size
450 as follows:

451 $$N_j = \left(2s_j^2 p_j(1-p_j)\right)^{-1}$$

452 where s_j is the standard error of the log odds ratio, and p_j is the effect allele frequency
453 for variant j. For imputed variants, we adjusted the effective sample size to account for
454 imputation uncertainty:

455 $$N_j = r_j^2 \left(2s_j^2 p_j(1-p_j)\right)^{-1}$$

456 where r_j^2 is the imputation quality score for variant j. To reduce the influence of poorly
457 powered variants, we excluded those with effective sample sizes in the lowest 10%
458 quantile and retained only the top 90% for heritability analysis. To assess the
459 robustness of our heritability estimates, we conducted sensitivity analyses using varying
460 SNP inclusion criteria, including: 1) using variants present in HapMap3 alone versus
461 variants in HapMap3 plus the MEGA array, and 2) varying the MAF thresholds of
462 between MAF > 0.01 or MAF > 0.05.

463 **Assessing polygenicity of breast cancer across samples**

464 To assess the polygenicity of genetic effects of breast cancer risk within each sample,
465 we utilized the GENESIS framework[21,22], which models GWAS summary statistics under
466 a three-component mixture model. Analyses were constrained to variants with MAF >
467 0.05 and in HapMap3 panel, following the guidance from GENESIS. For EUR and EAS

468 samples, we used the precomputed LD provided by GENESIS. For the AFR and H/L
469 samples, we constructed ancestry-specific LD-scores using individuals from the 1000G
470 AMR samples, and the 2730 AA controls from AABCG, as described in the heritability
471 analysis section. Following GENESIS's guidance, LD scores were computed by defining
472 tagging variants as those within a 1Mb window size and with an estimated LD
473 coefficient r^2 above 0.1. GENESIS models the distribution of genetic marker effect sizes
474 using a mixture of three components, including two normal distributions for non-null
475 genetic markers with distinct variance components. This allows the model to capture
476 both highly polygenic background signals and a subset of genetic markers with larger
477 effect sizes. From the fitted model, we estimated the total number of susceptibility
478 genetic markers with non-zero effect sizes. We also calculated the proportion of logit-
479 scale heritability explained by a CT-PRS. The CT-PRS[23,24] is a commonly used method
480 that selects approximately independent variants through LD clumping and optimizes p-
481 value thresholds to maximize predictive performance. Finally, we projected the
482 expected AUC for CT-PRS at varying GWAS sample sizes based on the model
483 estimates.

484 **Examining genetic correlations of breast cancer risk between samples**

485 To estimate cross-sample genetic correlations in breast cancer risk, we utilized the
486 Popcorn package[25]. Cross-ancestry LD reference panels were built from the same
487 ancestry-specific sources used in heritability analyses. We applied a MAF filter >0.01 for
488 EUR, EAS, and AFR samples, and >0.05 for the H/L sample to ensure robustness in LD
489 estimation. We then utilized the default settings in Popcorn to compute pairwise, cross-
490 sample genetic correlations for 1) variants in the HapMap3 reference panel and 2) the
491 combined set of HapMap3 and MEGA array variants.

492 **Genomic enrichment analysis using stratified LD-score regression**

493 We used S-LDSC to estimate the contribution of functional genomic annotations to
494 SNP-based heritability of breast cancer[26,27]. S-LDSC models GWAS test statistics as a
495 function of LD to variants in annotated regions, allowing partitioning of heritability while
496 accounting for LD structure and overlapping annotations. We used 73 binary

497 annotations from the baseline-LD v2.2 model[26–28], which includes regulatory, coding,
498 and evolutionary features compiled from ENCODE, Roadmap Epigenomics, and
499 comparative genomics data. Key annotations discussed in the Results include:

500 1. Ancient promoters: Promoter elements whose sequence aligns to species that
501 diverged before the placental–marsupial split, representing deeply conserved regulatory
502 regions[28].

503 2. TFBS: Genomic regions identified from aggregated ENCODE ChIP-seq[47] and DNase
504 I footprinting data[48], representing sites of transcription factor occupancy.

505 3. H3K4me3: A histone modification marking active promoter regions, aggregated
506 across tissues from ENCODE[47] and Roadmap Epigenomics[49].

507 4. H3K4me1: A mark associated with primed or poised enhancers[27].

508 5. H3K27ac: A mark of active enhancers and promoters[27].

509 6. Super-enhancers: Large regulatory domains composed of clustered enhancers with
510 high H3K27ac signal intensity[50].

511 We restricted analyses to SNPs from the HapMap3 panel with minor allele
512 frequency >5%. For EUR and EAS, we used precomputed LD scores
513 (https://zenodo.org/records/10515792). For AFR and H/L, we computed ancestry-
514 specific LD scores using reference samples from the AABCG consortium (AFR) and
515 1000 Genomes AMR (H/L), combining annotations from EUR and EAS sources.
516 Enrichment was defined as the proportion of heritability explained by SNPs in each
517 annotation divided by the proportion of SNPs overlapping that annotation.

518 **Cell-type specific associations analysis using scDRS+**

519 To identify cell types associated with breast cancer risk, we applied scDRS+[29,30], an
520 improved version of scDRS[30] with enhanced accuracy through single-cell imputation
521 and modeling of associations among related cell populations, to GWAS summary
522 statistics from each ancestry alongside the Tabula Sapiens scRNA-seq atlas[31] (27,051
523 cells from 133 cell types across 24 tissues; 50 cell types with >100 cells). This included
524 580 cells from the mammary tissue (cell types with >100 cells: luminal epithelial cells of

525 mammary gland, T cells, fibroblast of breast), and immune cell types (cell types
526 with >300 cells across all tissues: macrophage, CD8-positive, alpha-beta T cell, CD4-
527 positive, alpha-beta T cell, memory B cell, monocyte, plasma cell, B cell, T cell, classical
528 monocyte, NK cell, innate lymphoid cell, immune cell, CD8-positive, alpha-beta memory
529 T cell, neutrophil, CD4-positive, alpha-beta memory T cell, naive thymus-derived CD4-
530 positive, alpha-beta T cell).

531 To enhance data quality, we restricted analyses to fluorescence-activated cell-sorting
532 cells. For each ancestry, we incorporated the top 1,000 MAGMA-prioritized genes[51] into
533 the scDRS+ framework to calculate cell-level disease relevance scores. We first
534 identified marginally associated cells using an FDR threshold of 0.1 (analogous to
535 scDRS), followed by joint fine-mapping to identify cells associated with breast cancer
536 across ancestries. Cell-type-disease enrichments were tested by aggregating cell-level
537 scores (marginal and joint) following the scDRS pipeline[30].

538 To evaluate cross-sample concordance, we calculated the correlation of scDRS+
539 marginal scores between each pair of ancestries across all cells in a given cell type. We
540 compared these to an empirical null distribution derived from control scores to obtain p-
541 values for significant nonzero correlation. For all analyses, variant sets were restricted
542 to HapMap3 + MEGA SNPs, using MAF > 0.01 for AFR, EAS, and EUR, and MAF >
543 0.05 for H/L.

REFERENCES

1. Sung, H. *et al.* Global Cancer Statistics 2020: GLOBOCAN Estimates of Incidence and Mortality Worldwide for 36 Cancers in 185 Countries. *CA Cancer J. Clin.* **71**, 209–249 (2021).
2. Jia, G. *et al.* Genome- and transcriptome-wide association studies of 386,000 Asian and European-ancestry women provide new insights into breast cancer genetics. *Am. J. Hum. Genet.* **109**, 2185–2195 (2022).
3. Adedokun, B. *et al.* Cross-ancestry GWAS meta-analysis identifies six breast cancer loci in African and European ancestry women. *Nat. Commun.* **12**, (2021).
4. Zhang, H. *et al.* Genome-wide association study identifies 32 novel breast cancer susceptibility loci from overall and subtype-specific analyses. *Nat. Genet.* **52**, 572–581 (2020).
5. Michailidou, K. *et al.* Genome-wide association analysis of more than 120,000 individuals identifies 15 new susceptibility loci for breast cancer. *Nat. Genet.* **47**, 373–380 (2015).
6. Michailidou, K. *et al.* Large-scale genotyping identifies 41 new loci associated with breast cancer risk. *Nat. Genet.* **45**, 353–361 (2013).
7. Michailidou, K. *et al.* Association analysis identifies 65 new breast cancer risk loci. *Nature* **551**, 92–94 (2017).
8. Shu, X. *et al.* Identification of novel breast cancer susceptibility loci in meta-analyses conducted among Asian and European descendants. *Nat. Commun.* **11**, 1–9 (2020).
9. Han, M. R. *et al.* Genome-wide association study in East Asians identifies two novel breast cancer susceptibility loci. *Hum. Mol. Genet.* **25**, 3361 (2016).
10. Feng, Y. *et al.* A comprehensive examination of breast cancer risk loci in African American women. *Hum. Mol. Genet.* **23**, 5518–5526 (2014).
11. Huo, D. *et al.* Genome-wide association studies in women of African ancestry identified 3q26.21 as a novel susceptibility locus for estrogen receptor negative breast cancer. *Hum Mol Genet.* **25**, 4835–4846 (2016).
12. Jia, G. *et al.* Genome-wide association analyses of breast cancer in women of African ancestry identify new susceptibility loci and improve risk prediction. *Nat. Genet.* **56**, 819–826 (2024).
13. Hayat, M. *et al.* Genome-wide association study identifies common variants associated with breast cancer in South African Black women. *Nat. Commun.* **16**, 3542 (2025).
14. Hoffman, J. *et al.* Identification of novel common breast cancer risk variants at the 6q25 locus among Latinas 06 Biological Sciences. *Breast Cancer Res.* **21**, (2019).
15. Fejerman, L. *et al.* Genome-wide association study of breast cancer in Latinas identifies novel protective variants on 6q25. *Nat. Commun.* **5**, 1–8 (2014).
16. Roberts, E., Howell, S. & Evans, D. G. Polygenic risk scores and breast cancer risk prediction. *Breast* **67**, 71–77 (2023).
17. Bulik-Sullivan, B. K. *et al.* LD Score regression distinguishes confounding from polygenicity in genome-wide association studies. *Nat. Genet.* **47**, 291–295 (2015).
18. Altshuler, D. M. *et al.* Integrating common and rare genetic variation in diverse human populations. *Nature* **467**, 52–58 (2010).

587 19. Bien, S. A. *et al.* Strategies for Enriching Variant Coverage in Candidate Disease Loci on
588 a Multiethnic Genotyping Array. *PLoS One* **11**, 167758 (2016).
589 20. Auton, A. *et al.* A global reference for human genetic variation. *Nature* **526**, 68–74 (2015).
590 21. Zhang, Y., Qi, G., Park, J. H. & Chatterjee, N. Estimation of complex effect-size
591 distributions using summary-level statistics from genome-wide association studies across
592 32 complex traits. *Nat. Genet.* **50**, 1318–1326 (2018).
593 22. Zhang, Y. D. *et al.* Assessment of polygenic architecture and risk prediction based on
594 common variants across fourteen cancers. *Nat. Commun.* **11**, 1–13 (2020).
595 23. Purcell, S. M. *et al.* Common polygenic variation contributes to risk of schizophrenia and
596 bipolar disorder. *Nature* **460**, 748–752 (2009).
597 24. Wray, N. R., Goddard, M. E. & Visscher, P. M. Prediction of individual genetic risk to
598 disease from genome-wide association studies. *Genome Res.* **17**, 1520–1528 (2007).
599 25. Brown, B. C., Ye, C. J., Price, A. L. & Zaitlen, N. Transethnic Genetic-Correlation
600 Estimates from Summary Statistics. *Am. J. Hum. Genet.* **99**, 76–88 (2016).
601 26. Gazal, S. *et al.* Linkage disequilibrium-dependent architecture of human complex traits
602 shows action of negative selection. *Nat. Genet.* **49**, 1421–1427 (2017).
603 27. Finucane, H. K. *et al.* Partitioning heritability by functional annotation using genome-wide
604 association summary statistics. *Nat. Genet.* https://doi.org/10.1038/ng.3404 (2015)
605 doi:10.1038/ng.3404.
606 28. Hujoel, M. L. A., Gazal, S., Hormozdiari, F., van de Geijn, B. & Price, A. L. Disease
607 Heritability Enrichment of Regulatory Elements Is Concentrated in Elements with Ancient
608 Sequence Age and Conserved Function across Species. *Am. J. Hum. Genet.* **104**, 611–
609 624 (2019).
610 29. Turcan, A., Zhang, M. & Hou, K. Accurate polygenic association of disease to individual
611 cells in single-cell RNA-seq data. in *Presented at: American Society of Human Genetics*
612 *(ASHG) Annual Meeting* (2024).
613 30. Zhang, M. J. *et al.* Polygenic enrichment distinguishes disease associations of individual
614 cells in single-cell RNA-seq data. *Nat. Genet.* **54**, 1572–1580 (2022).
615 31. Jones, R. C. *et al.* The Tabula Sapiens: A multiple-organ, single-cell transcriptomic atlas
616 of humans. *Science (1979)* **376**, (2022).
617 32. Zheng, C. *et al.* Neutrophils in triple-negative breast cancer: an underestimated player
618 with increasingly recognized importance. *Breast Cancer Res.* **25**, (2023).
619 33. Obeagu, E. I. & Obeagu, G. U. Exploring neutrophil functionality in breast cancer
620 progression: A review. *Medicine (United States)* **103**, E37654 (2024).
621 34. Camargo, S. *et al.* Neutrophils physically interact with tumor cells to form a signaling
622 niche promoting breast cancer aggressiveness. *Nat. Cancer* **6**, (2025).
623 35. Zhao, Y. *et al.* Neutrophils resist ferroptosis and promote breast cancer metastasis
624 through aconitate decarboxylase 1. *Cell Metab.* **35**, 1688-1703.e10 (2023).
625 36. Wang, Y. H. *et al.* Monocytes secrete CXCL7 to promote breast cancer progression. *Cell*
626 *Death Dis.* **12**, (2021).
627 37. Kresovich, J. K. *et al.* Prediagnostic Immune Cell Profiles and Breast Cancer. *JAMA*
628 *Netw. Open* **3**, (2020).
629 38. Hou, K. *et al.* Admix-kit: an integrated toolkit and pipeline for genetic analyses of admixed
630 populations. *Bioinformatics* **40**, (2024).

631 39. Zhong, Y., Perera, M. A. & Gamazon, E. R. On Using Local Ancestry to Characterize the
632 Genetic Architecture of Human Traits: Genetic Regulation of Gene Expression in
633 Multiethnic or Admixed Populations. *Am. J. Hum. Genet.* **104**, 1097–1115 (2019).
634 40. Yang, Z. *et al.* Fine-mapping in admixed populations using CARMA-X, with applications
635 to Latin American studies. *Am. J. Hum. Genet.*
636 https://doi.org/10.1016/J.AJHG.2025.02.020, (2025) doi:10.1016/J.AJHG.2025.02.020,.
637 41. Pharoah, P. D. P. *et al.* Polygenic susceptibility to breast cancer and implications for
638 prevention. *Nat. Genet.* **31**, 33–36 (2002).
639 42. Gao, G. *et al.* Polygenic risk scores for prediction of breast cancer risk in women of
640 African ancestry: a cross-ancestry approach. *Hum. Mol. Genet.* **31**, 3133–3143 (2022).
641 43. McEvoy, B. P., Powell, J. E., Goddard, M. E. & Visscher, P. M. Human population
642 dispersal 'Out of Africa' estimated from linkage disequilibrium and allele frequencies of
643 SNPs. *Genome Res.* **21**, 821–829 (2011).
644 44. Hagerling, C. *et al.* Immune effector monocyte–neutrophil cooperation induced by the
645 primary tumor prevents metastatic progression of breast cancer. *Proc. Natl. Acad. Sci.*
646 **116**, 21704–21714 (2019).
647 45. Sakaue, S. *et al.* A cross-population atlas of genetic associations for 220 human
648 phenotypes. *Nat. Genet.* **53**, 1415–1424 (2021).
649 46. Gazal, S., Sahbatou, M., Babron, M. C., Genin, E. & Leutenegger, A. L. High level of
650 inbreeding in final phase of 1000 Genomes Project. *Sci. Rep.* **5**, (2015).
651 47. Dunham, I. *et al.* An integrated encyclopedia of DNA elements in the human genome.
652 *Nature* **489**, 57–74 (2012).
653 48. Trynka, G. *et al.* Chromatin marks identify critical cell types for fine mapping complex trait
654 variants. *Nat. Genet.* **45**, 124–130 (2012).
655 49. Roadmap Epigenomics Consortium *et al.* Integrative analysis of 111 reference human
656 epigenomes. *Nature* **518**, 317–329 (2015).
657 50. Hnisz, D. *et al.* Super-enhancers in the control of cell identity and disease. *Cell* **155**, 934
658 (2013).
659 51. de Leeuw, C. A., Mooij, J. M., Heskes, T. & Posthuma, D. MAGMA: Generalized Gene-
660 Set Analysis of GWAS Data. *PLoS COMPUT. Biol.* **11**, (2015).
661

662 **ACKNOWLEDGEMENTS**

663 The analysis utilized DNANexus and the high-performance computation Biowulf cluster
664 at the National Institutes of Health (NIH), USA. L.C-C. is grateful for financial support
665 from NIH (grants R56CA280636, D43CA260689, U54CA233306, U54CA283766 and
666 U54CA280811) and The Heart, BrEast, and BrAin HeaLth Equity Research (HEAL
667 HER) program, a program made possible by residual class settlement funds in the
668 matter of April Krueger v. Wyeth, Inc., Case No. 03-cv-2496 (US District Court, SD of
669 Calif.). J.Weitzel is supported by the Breast Cancer Research Foundation (grant 24-

210). COLUMBUS acknowledgements are available in **Supplementary**

Acknowledgement. This research was supported in part by the Intramural Research Program of the NIH. The contributions of the NIH authors were made as part of their official duties as NIH federal employees, are in compliance with agency policy requirements, and are considered Works of the United States Government. However, the findings and conclusions presented in this paper are those of the authors and do not necessarily reflect the views of the NIH or the U.S. Department of Health and Human Services.

AUTHOR CONTRIBUTIONS

T.U.A and H.Z. conceived the project. J.L.L. and J.Williams conducted the heritability analyses. J.W., Q.H. and L.Y. conducted the polygenicity analyses. O.J. conducted the cross-sample genetic correlation analyses. J.Williams and M.Z. conducted the enrichment analyses. A.T. conducted scDRS+ analyses. J.W. computed the LD-scores for EAS, EUR and H/L. G.J. computed the LD-scores and MAGMA analyses on AABCG controls. Statistical analyses were conducted under the guidance of K.M., Q.Z., M.J.Z., D.D., T.U.A., and H.Z.; J.L.L., M.J.Z., J. Williams, O.J., A.T., T.U.A. and H.Z. wrote the first draft. J.T.B., L.F., W.Z., S.J.C., N.C., P.K., M.G.C., M.J.Z., T.U.A and H.Z. reviewed and edited the draft. All co-authors reviewed and approved the final version of the manuscript.

DATA AVAILABILITY

AFR GWAS summary statistics are available at GWAS Catalog (GCST90296719)

BCAC EAS GWAS summary statistics are available at:
https://www.ccge.medschl.cam.ac.uk/breast-cancer-association-consortium-bcac/data-data-access/summary-results/gwas-summary-results

Biobank Japan GWAS summary statistics are available at: https://pheweb.jp/pheno/BrC

BCAC EUR GWAS summary statistics are available at:
https://www.ccge.medschl.cam.ac.uk/breast-cancer-association-consortium-bcac/data-data-access/summary-results/gwas-summary-associations

The H/L GWAS summary statistics are available by contacting Dr. Elad Ziv (elad.ziv@ucsf.edu) to gain access.

CODE AVAILABILITY

All data analysis code is available at: https://github.com/confluence-breast-cancer-consortia/pre-confluence-analysis/tree/main

LDSC and stratified LDSC are available at: https://github.com/bulik/ldsc

GENESIS is available at: https://github.com/yandorazhang/GENESIS

Popcorn is available at: https://github.com/brielin/Popcorn

scDRS is available at: https://github.com/martinjzhang/scDRS